

# Charge and spin order on the triangular lattice — $\text{Na}_x\text{CoO}_2$ at $x = 0.5$

Sen Zhou and Ziqiang Wang

*Department of Physics, Boston College, Chestnut Hill, MA 02467*

(Dated: December 2, 2024)

The nature of charge and spin order of strongly correlated triangular lattice fermions is investigated in connection to the unconventional insulating state of  $\text{Na}_x\text{CoO}_2$  at  $x = 0.5$ . We study an extended Hubbard ( $t$ - $U$ - $V$ ) model of the electron doped Co  $a_{1g}$  band using a spatially unrestricted Gutzwiller approximation. We find a new class of charge and spin ordered states at  $x = 1/3$  and  $x = 0.5$  where the system alleviates antiferromagnetic (AF) frustration via charge inhomogeneity. We show that the  $\sqrt{3}a \times 2a$  off-plane Na dopant order at  $x = 0.5$  plays an important but subtle role. It induces weak  $\sqrt{3}a \times 1a$  charge order in the Co layer without gapping the Fermi surface and allows successive  $\sqrt{3}a \times 1a$  AF and  $2a \times 2a$  charge/spin ordering transitions at low temperatures. The nesting with the  $2a \times 2a$  hexagonal zone boundary gaps out almost the entire Fermi surface at  $x = 0.5$ . We study the phase structure and compare to the findings of recent experiments.

PACS numbers: 71.27.+a, 71.18.+y, 74.25.Jb, 74.70.-b

Sodium doped cobaltate  $\text{Na}_x\text{CoO}_2$  has emerged recently as an important, layered triangular lattice fermion system with a rich phase structure [1]. These include a 5K superconducting phase near  $x = 1/3$  upon hydration [2]; an A-type antiferromagnetic (AF) phase around  $x = 0.8$  [3]; and an unexpected insulating state at  $x = 0.5$  [1]. A series of experiments find the insulating state unconventional. While the magnetic susceptibility shows two cusps at  $T_{m1} = 88\text{K}$  and  $T_{m2} = 53\text{K}$ , the in-plane resistivity exhibits only a derivative feature at  $T_{m1}$ , followed by a metal-insulator transition near  $T_{m2}$  [1]. The insulating state has a small optical gap of 15meV [4, 5] and a single-particle gap around 10meV measured by angle resolved photoemission spectroscopy (ARPES) [6]. Electron diffraction [7, 8] shows that Na atoms order into  $\sqrt{3}a \times 2a$  (hereafter we set  $a = 1$ ) supercells at  $x = 0.5$  below  $\sim 300\text{K}$ , suggesting that dopant order induced charge order may play a role in the insulating behaviors [1, 4, 9]. However, NMR experiments find that the Co valence exhibits small disproportionation with no appreciable change across the metal-insulator transition [10]. Bobroff et al. proposed that the insulating state is a result of successive SDW transitions due to the nesting of the Fermi surface (FS) with the orthorhombic zone boundary of  $\sqrt{3} \times 2$  dopant order [10]. Most recently, elastic neutron scattering discovered that AF order occurs at  $T_{m1}$  with a  $2 \times 2$  hexagonal unit cell [11]. The ordering vector is clearly incompatible with the nesting wavevectors of the orthorhombic zone boundary and challenges the SDW scenario.

In this paper, we address the nature of charge and spin order at  $x = 0.5$  through microscopic calculations. The relevant low energy electronic structure involves three Co  $t_{2g}$  atomic orbitals forming one  $a_{1g}$  and two  $e_g'$  bands in the solid. LDA calculations predicted a large FS associated with the  $a_{1g}$  and six small FS pockets of mostly  $e_g'$  character [12]. However, ARPES measurements find that only the  $a_{1g}$  band crosses the Fermi level, giving rise to a

single FS, while the  $e_g'$  bands lie below the Fermi level for a wide range of Na doping  $x$  [13, 14, 15]. The same conclusion was reached by ARPES in hydrated samples [16]. In a recent work [17], starting from a three-band Hubbard model of the  $t_{2g}$  complex with LDA band dispersions, we have shown that strong correlations can drive the  $e_g'$  band below the Fermi level as observed by ARPES. In this sense, a single-band model for the essential low energy physics is justified, provided that the strong local Coulomb repulsion is considered at the Co site.

We consider here a single-band Hubbard ( $t$ - $U$ - $V$ ) model of the  $a_{1g}$  band with long-range Coulomb interaction  $V$  and study the interplay between the frustration of the kinetic energy due to strong correlation and that of the AF spin correlations on the triangular lattice. Specifically, we extend the Gutzwiller approximation to the variational space spanned by spatially unrestricted and spin dependent renormalization factors. We find that the tendency towards inhomogeneity due to strong correlation and magnetic frustration work together to alleviate the AF frustration and produce a class of charge and spin ordered states. At  $x = 1/3$ , the ground state has spontaneous  $\sqrt{3} \times \sqrt{3}$  charge and spin order even when  $V = 0$ . The frustration is avoided as the moments order antiferromagnetically on the honeycomb lattice and coexist with weak charge density modulations. At  $x = 0.5$ , we find that a large  $V$  greater than a critical value is necessary to destabilize the uniform paramagnetic phase towards a state with  $\sqrt{3} \times 1$  charge and AF spin order. This state is close to a Wigner crystal with a large charge disproportionation and a large insulating gap [18, 19], inconsistent with NMR [10], transport [1, 4, 5], and ARPES [6] experiments. We show that the  $\sqrt{3} \times 2$  Na order at  $x = 0.5$  induces a weak  $\sqrt{3} \times 1$  charge order at high temperatures without affecting the FS. The hexagonal symmetry breaking allows  $\sqrt{3} \times 1$  AF order to develop at  $T_{m1}$ . Interestingly, we find that the  $2 \times 2$  hexagonal zone boundary is well nested with the FS at  $x = 0.5$ , allowing  $2 \times 2$

charge and spin order to develop at a lower temperature  $T_{m2}$  and giving rise to an insulating ground state.

We begin with the one-band  $t$ - $U$ - $V$  model

$$H = \sum_{ij\sigma} t_{ij} c_{i\sigma}^\dagger c_{j\sigma} + U \sum_i \hat{n}_{i\uparrow} \hat{n}_{i\downarrow} + V \sum_{i>j} \frac{\hat{n}_i \hat{n}_j}{|\vec{r}_i - \vec{r}_j|}, \quad (1)$$

where,  $c_{i\sigma}^\dagger$  creates an  $a_{1g}$  hole of spin  $\sigma$ ,  $\hat{n}_i$  is the hole density operator,  $U$  and  $V$  are the on-site and long-range Coulomb repulsion. From the LDA  $a_{1g}$  band dispersion, the hopping parameters are chosen according to  $t_{ij} = (-202, 35, 29)$  meV for the first, second, and third nearest neighbors on the triangular lattice, respectively. The local electron density is given by  $1 + x_i$ , where  $x_i = 1 - n_i$  is the local electron doping concentration. The large- $U$  limit of Eq. (1) is usually treated in the Gutzwiller approximation (GA) [20, 21], which corresponds to the saddle point of the slave-boson path integral formulation of Kotliar and Ruckenstein [22]. To encompass the Hilbert space with inhomogeneous charge/spin densities, we adopt a spatially unrestricted GA,

$$H_{GW} = \sum_{ij\sigma} g_{ij}^\sigma t_{ij} c_{i\sigma}^\dagger c_{j\sigma} + \sum_{i,\sigma} \varepsilon_{i\sigma} (c_{i\sigma}^\dagger c_{i\sigma} - n_{i\sigma}) + V \sum_{i>j} \frac{\hat{n}_i \hat{n}_j}{|\vec{r}_i - \vec{r}_j|}, \quad (2)$$

where the Gutzwiller renormalization factor  $g_{ij}^\sigma$  depends on the sites connected by the hopping integral  $t_{ij}$  and on the spin of the hopping electron,

$$g_{ij}^\sigma = \sqrt{\frac{x_i x_j}{(1 - n_{i\sigma})(1 - n_{j\sigma})}}. \quad (3)$$

The  $\varepsilon_{i\sigma}$  in Eq. (2) is a spin dependent local fugacity that maintains the equilibrium condition and the local densities upon Gutzwiller projection [23, 24]. It is determined by  $\varepsilon_{i\sigma} = \partial \langle H_{GW} \rangle / \partial n_{i\sigma}$ . The spin density is  $S_i^z = (n_{i\uparrow} - n_{i\downarrow})/2$ . We note in passing that if the charge density is forced to be uniform, the solution of Eq. (2) gives a stable paramagnetic phase up to  $x_0 \simeq 0.67$  where a ferromagnetic (FM) transition takes place. The AF phase, typical of large- $U$  systems at small  $x$  on bipartite lattices [22], is absent due to frustration on the triangular lattice. We find that this frustration can be alleviated by forming inhomogeneous electronic states.

To this end, we consider large triangular lattices of  $240 \times 320$  sites with  $6 \times 8$  unit cells wherein  $x_i$ ,  $n_{i\sigma}$ , and  $\varepsilon_{i\sigma}$  are allowed to have spatial variations and their values determined self-consistently by standard iterations. First let's consider the case at  $x = 1/3$ . It is remarkable that even for  $V = 0$  the ground state has spontaneous  $\sqrt{3} \times \sqrt{3}$  charge and spin order displayed in Fig. 1a. Frustration is alleviated as AF moments reside on the underlying unfrustrated honeycomb lattice. The tendency to avoid AF frustration is materialized because the FS at  $x = 1/3$  is

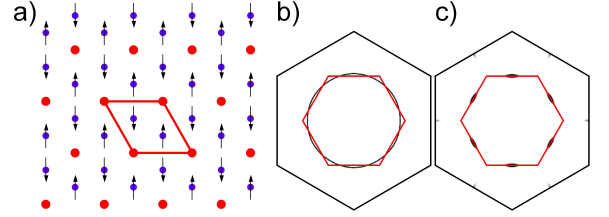


FIG. 1: (a)  $\sqrt{3} \times \sqrt{3}$  charge and spin order at  $x = 1/3$  and  $V = 0$ . The charge and spin densities are  $x = (0.32, 0.36, 0.32)$  and  $S^z = (0.18, 0.00, -0.18)$ . (b) Nesting of  $\sqrt{3} \times \sqrt{3}$  zone boundary with the paramagnetic FS. (c) Intensity of the quasiparticle peaks at the Fermi level.

well nested with the  $\sqrt{3} \times \sqrt{3}$  zone boundary, as shown in Fig. 1b, such that  $2k_f$  is nearly identical to the fluctuation vector directed to the original zone corners. This allows weak charge order to develop by “umklapp” scattering and anisotropic gapping of the FS shown in Fig. 1c. We find that charge and spin sectors are coupled in the sense that the removal of inhomogeneity in either will reinstate the uniform paramagnetic phase. This state is thus different from the  $\sqrt{3} \times \sqrt{3}$  CDW state proposed by Motrunich and Lee [25, 26] near  $x = 1/3$ , which results from Coulomb jamming due to a large  $V$ . In contrast, this ordered state has a very small insulating gap at  $V = 0$  which increases gradually with increasing  $V$ . We point out that such a spin/charge ordered state has not yet been observed at  $x = 1/3$ , most likely because of the disorder of the Na dopants [27]. It will be interesting to examine whether enhanced AF fluctuations in proximity to this ordered state can lead to singlet superconductivity.

Next we turn to  $x = 0.5$ , which is not a natural commensurate filling on the triangular lattice. As a result, the uniform paramagnetic state is found to be stable for small  $V < V_c$ ,  $V_c \simeq 1.35$  eV. For  $V > V_c$ , we find a first order transition to an inhomogeneous state with charge/spin order. Fig. 2 shows that, at  $V = 1.5$  eV, the moments are ordered into unfrustrated AF chains that are AF coupled and separated by nonmagnetic chains. This state is driven by strong long-range Coulomb  $V$  and stabilized by AF spin correlations. The charge density has a  $\sqrt{3} \times 1$  unit cell with strong disproportionation close to the  $\text{Co}^{3+}/\text{Co}^{4+}$  configuration, resulting in a large charge gap. Indeed, similar “AF Wigner crystal” was recently proposed [19] and independently investigated by variational Monte Carlo on small frustrated lattices [18]. It is important to note that while the spin configuration of the  $\sqrt{3} \times 1$  AF order, its unit cell and the magnetic zone match that deduced from neutron scattering of a  $2 \times 2$  hexagonal unit cell, the structure factor is different such that the magnetic Bragg peaks shown in Fig. 2 (green squares) only has two-fold symmetry. This differs from the hexagonal Bragg peaks observed in neutron scattering, unless 120 degree orientated domains of equal contribution are present [11]. For this reason, we will continue to refer to this spin pattern as  $\sqrt{3} \times 1$  AF order (see also

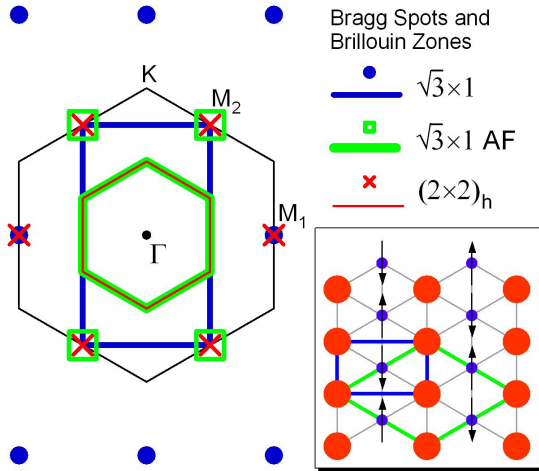


FIG. 2:  $\sqrt{3} \times 1$  charge and AF spin order at  $x = 0.5$  and  $V = 1.5\text{eV}$  (lower right). The charge and spin densities:  $x = (0.05, 0.95, 0.05)$  and  $S^z = (0.48, 0.00, -0.48)$ . Also shown are charge and magnetic zones and Bragg peak locations of different structures. Note the absence of Bragg spot at  $M_1$  for  $\sqrt{3} \times 1$  AF order.  $(2 \times 2)_h$  corresponds to the hexagonal magnetic zone and Bragg spots of the state shown in Fig. 3c.

Fig. 3b) and reserve the term  $2 \times 2$  hexagonal unit cell for a state with hexagonal Bragg peaks (see Fig. 3c). In view of the experimental findings of weak charge disproportionation by NMR [10], and small insulating gaps by transport, optics, and ARPES [1, 4, 6], we conclude that this state, though indicative of the structure of the AF order by avoiding frustration via inhomogeneity, cannot describe the  $x = 0.5$  phase of the cobaltates.

It turns out that the Na dopant order plays an important but subtle role at  $x = 0.5$ . Below about 300K, Na orders on the two preferred sites, forming  $\sqrt{3} \times 2$  superlattice structures [7, 8]. This has led to the notion of an induced  $\sqrt{3} \times 2$  electron charge order in the Co plane, which is ultimately responsible for the insulating state at  $x = 0.5$ . Three remarks are in order. First, the off-plane ionic dopant potential in transition metal oxides is usually not strong due to screening by phonons, interband transitions, and the mobile carriers. Thus, the induced charge order in the basal plane is at most moderate. Second, as temperature is lowered, FS stability may occur depending on the charge ordering symmetry. The latter can be different from the symmetry of dopant order. Due to the fact that the zigzag chains of ordered Na dopants above and below a Co layer are staggered, the superlattice potential felt by the electrons has a higher symmetry and results in  $\sqrt{3} \times 1$  charge order with a much elongated orthorhombic zone than originally thought. Third, the breaking of the lattice symmetry makes it energetically favorable to develop AF order by alleviating frustration via weak charge inhomogeneity.

The effect of the Na dopant potential is to add

$$V_{\text{dopant}}(i) = V_d \sum_{I=1}^{N_{\text{Na}}} \frac{\hat{n}_i}{\sqrt{|\vec{r}_I - \vec{r}_i|^2 + d_z^2}} \quad (4)$$

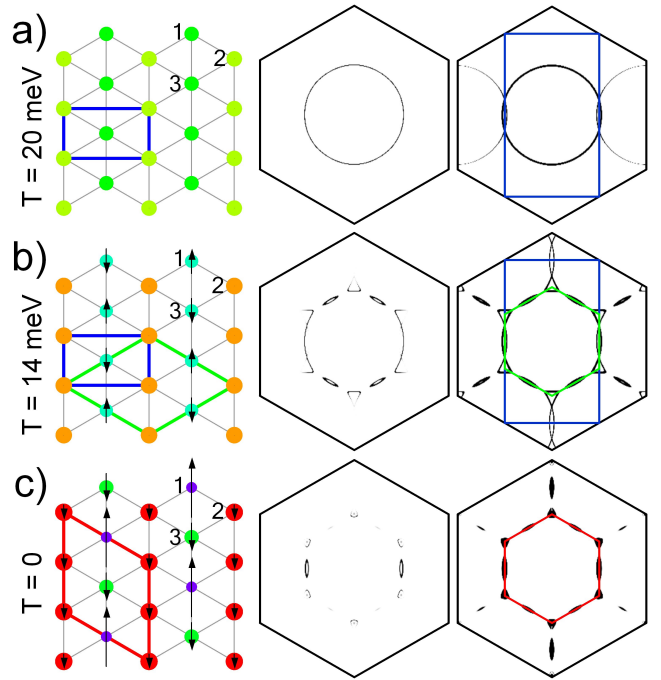


FIG. 3: The self-consistent states at  $x = 0.5$  for three different temperatures (a), (b), and (c). First column: charge/spin ordering patterns and the unit cells. Second column: FS without thermal broadening showing the anisotropic gapping of the FS. Third column: FS when intensity scale is reduced by four orders of magnitude showing the band folding along zone boundaries of corresponding charge/spin order.

to Eq. (2), where  $V_d$  is the potential strength and  $d_z \simeq a$  is the setback distance of Na to the Co plane. Not to discriminate against carrier screening of the dopant potential, the long-range Coulomb  $V$  is set to be the same as  $V_d$ , and  $V = V_d = 0.2\text{eV}$  is used in the calculation. We present the temperature evolution of the self-consistently determined states in Fig. 3, and that of the charge and spin density in Fig. 4. At a temperature  $k_B T = 20\text{meV}$  above  $T_{m1}$  marked in Fig. 4, the electronic state shown in Fig. 3a has  $\sqrt{3} \times 1$  charge order induced by the Na potential *without* magnetic order. Note that the charge modulation shown in Fig. 4 is weak (1.6%) such that the FS in Fig. 3a is not affected. Lowering of the intensity scale by four orders of magnitude reveals the weak band folding patterns along the intersections of the FS with the  $\sqrt{3} \times 1$  zone boundary. As the temperature is lowered, we find an AF transition at  $T_{m1}$  marked in Fig. 4, below which  $\sqrt{3} \times 1$  AF order develops and coexists with the  $\sqrt{3} \times 1$  charge order. This state is shown in Fig. 3b at  $k_B T = 14\text{meV}$ . The transition is primarily a spin ordering transition, involving small changes in charge disproportionation ( $\sim 4\%$  from Fig. 4). This is consistent with NMR measurements [10]. Remarkably, Fig. 3b shows that the FS at  $x = 0.5$  is well nested with the hexagonal magnetic zone boundary. However, since the structure factor of the  $\sqrt{3} \times 1$  AF order breaks the hexagonal symmetry, the nested vertical sections of the

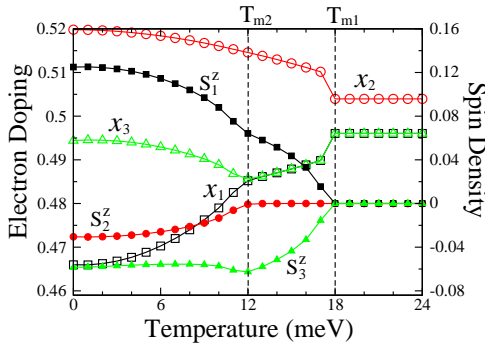


FIG. 4: Temperature evolution of charge (electron doping) and spin densities at three sites marked in Fig. 3. The spin/charge ordering transitions are marked by  $T_{m1}$  and  $T_{m2}$ .

FS remain intact as the  $2k_f$  scattering between them is switched off by the absence of a magnetic Bragg peak at  $M_1$  shown in Fig. 2. Thermal broadening of the small gaps associated with the weak truncation of the FS and the 120 degree domains may weaken the features of  $T_{m1}$  in resistivity, optics, and ARPES measurements. Nevertheless, the topology change, the emergence of electron-like FS pockets, may lead to the reduction observed in the Hall number [1] below  $T_{m1}$ .

Reducing the temperature further, we find a second transition marked as  $T_{m2}$  in Fig. 4 associated with additional symmetry breaking. Below  $T_{m2}$ , small magnetic moments develop at the Co(2) sites. They are coupled *ferromagnetically* as shown in Fig. 3c at  $T = 0$ . Below  $T_{m2}$ , the charge and spin densities in Fig. 4 are all different on the three inequivalent Co sites. Hence the ground state has charge and spin order with identical  $2 \times 2$  hexagonal unit cell. Moreover, the Fourier transform of the spin density has now hexagonal Bragg peaks in a single domain (see Fig. 2) of similar weight at low temperatures. As a result of the combined  $2 \times 2$  charge/spin order, the “ $2k_f$ ” scattering destroys almost the entire nested FS as shown in Fig. 3c, giving rise to the onset of the metal-insulator transition below  $T_{m2}$ . The residual incomplete electron-like and hole-like FS pockets have six-fold symmetry with a two-fold anisotropy. Although the volume of these pockets are somewhat smaller compared to the pockets detected by high-field Shubnikov-de Haas oscillations [28], the insulating state has a nonzero density of states, and in this sense a pseudogap. We emphasize that the most important character of the transition at  $T_{m2}$  is the emergence of small moments at Co(2). Its ordering direction and the size of the moments, in particular at Co(1) and Co(3), should not be taken literally since it is specific to the restriction to collinear spins in the Gutzwiller approach. It can be more energetically favorable for the small moment to point along  $c$ -axis to avoid frustration of the in-plane AF order. Recent NMR experiments [29, 30] at  $x = 0.5$  are consistent with the ordering of such small moments below the 53K transition.

To summarize, we have shown that the unconventional

insulating state at  $x = 0.5$  is a result of the interplay among strong correlation, AF order by alleviating frustration via inhomogeneity, weak  $\sqrt{3} \times 1$  charge order induced by Na dopant order, and the nesting of the FS with the  $2 \times 2$  hexagonal magnetic zone boundary. A single band Hubbard model including the Na dopant potential for the electron doped, hole-like Co  $a_{1g}$  band on the triangular lattice captures the basic physics of charge and spin order. The transition temperatures  $T_{m1}$  and  $T_{m2}$ , the size of the moments, and the insulating gap will depend on microscopic details such as the band parameters and the strength of the dopant potential  $V_d$ , and thus must vary when Na is replaced by other isoelectronic atoms such as potassium in  $K_{0.5}CoO_2$ . However, the phase structure discussed here is expected to be universal of the cobaltate family at  $x = 0.5$ .

We thank H. Ding, Y. S. Lee, and especially P.A. Lee for many valuable discussions. This work is supported by DOE grants DE-FG02-99ER45747 and ACS grant 39498-AC5M.

---

- [1] M.L. Foo et al., Phys. Rev. Lett. **92**, 247001 (2004).
- [2] K. Takada, et. al., Nature (London) **422**, 53 (2003).
- [3] S.P. Bayrakci et al., Phys. Rev. Lett. **94**, 157205 (2005).
- [4] N.L. Wang et al., Phys. Rev. Lett. **93**, 147403 (2004).
- [5] J. Hwang et al., Phys. Rev. B**72**, 024549 (2005).
- [6] D. Qian et al., Phys. Rev. Lett. **96**, 046407 (2006).
- [7] H.W. Zandbergen et al., Phys. Rev. B**70**, 024101 (2004).
- [8] Q. Huang et al., J. Phys. Cond. Matt. **16**, 5803 (2004).
- [9] K.-W. Lee et al., Phys. Rev. Lett. **94**, 026403 (2005).
- [10] J. Bobroff et al., Phys. Rev. Lett. **96**, 107201 (2006).
- [11] G. Gasparovic et al., Phys. Rev. Lett. **96**, 046403 (2006).
- [12] D.J. Singh, Phys. Rev. B**61**, 13397 (2000).
- [13] H.B. Yang et al., Phys. Rev. Lett. **95**, 146401 (2005).
- [14] M.Z. Hasan et al., Phys. Rev. Lett. **92**, 246402 (2004).
- [15] H.B. Yang et al., Phys. Rev. Lett. **92**, 246403 (2004).
- [16] T. Shimojima et. al., cond-mat/0606424.
- [17] S. Zhou et. al., Phys. Rev. Lett. **94**, 206401 (2005).
- [18] H. Watanabe and M. Ogata, J. Phys. Soc. Jpn. **75**, 063702 (2006).
- [19] T.P. Choy et. al., cond-mat/0502164.
- [20] D. Vollhardt, Rev. Mod. Phys. **56**, 99 (1984).
- [21] F.C. Zhang et al., Supercond. Sci. Techol. **1**, 36 (1998).
- [22] G. Kotliar and A.E. Ruckenstein, Phys. Rev. Lett. **57**, 1362 (1986).
- [23] C. Li et al., Phys. Rev. B**73**, 060501 (2006).
- [24] Q.-H. Wang et al., Phys. Rev. B**73**, 092507 (2006).
- [25] O.I. Motrunich and P.A. Lee, Phys. Rev. B**69**, 214516 (2004).
- [26] H. Watanabe and M. Ogata, J. Phys. Soc. Jpn. **74**, 2901 (2005).
- [27] D.J. Singh et. al., Phys. Rev. Lett. **97**, 016404 (2006).
- [28] L. Balicas et al., Phys. Rev. Lett. **94**, 236402 (2005).
- [29] T. Imai et al., cond-mat/0607625.
- [30] M. Yokoi et. al., J. Phys. Soc. Jpn. **74**, 3046 (2005).